doi:10.26443/seismica.v3i1.1084

Testing the Predictive Power of b Value for Italian Seismicity

Cataldo Godano [*1,2], **Anna Tramelli** [2], **Giuseppe Petrillo** [3,4], **Vincenzo Convertito** [2]

[1]Department of Mathematics and Physics, Università della Campania - Luigi Vanvitelli, Caserta, Italy., [2]Istituto Nazionale di Geofisica e Vulcanologia - Sezione di Napoli Osservatorio Vesuviano, Napoli, Italy., [3]The Institute of Statistical Mathematics, Research Organization of Information and Systems, Tokyo 106-8569, Japan., [4]Scuola Superiore Meridionale, Naples, Italy

Author contributions: *Conceptualization* Cataldo Godano, Vincenzo Convertito, Anna Tramelli. *Formal Analysis* Cataldo Godano, Vincenzo Convertito, Anna Tramelli, Giuseppe Petrillo. *Writing - Original draft* Cataldo Godano, Vincenzo Convertito, Anna Tramelli, Giuseppe Petrillo.

Abstract A very efficient method for estimating the completeness magnitude m_c and the scaling parameter b of earthquake magnitude distributions has been thoroughly tested using synthetic seismic catalogues. Subsequently, the method was employed to assess the capability of the b value in differentiating between foreshocks and aftershocks, confirming previous findings regarding the Amatrice-Norcia earthquake sequence. However, a blind algorithm reveals that the discriminative ability of the b value necessitates a meticulous selection of the catalogue, thereby reducing the predictability of large events occurring subsequent to a prior major earthquake.

Production Editor: Gareth Funning
Handling Editor: Andrea Llenos
Copy & Layout Editor: Anant Hariharan

Received: July 10th, 2023
Accepted: January 16th, 2024
Published: February 1st, 2024

1 Introduction

The exponential earthquake magnitude distribution, known as the Gutenberg and Richter (GR) law (Gutenberg and Richter, 1944), establishes that:

$$p(m) = b\ln(10)10^{-bm} \tag{1}$$

The scaling parameter b has been extensively investigated because it represents a primary instrument for the evaluation of the occurrence probability of an earthquake of a given size. Its value has been inversely correlated to the stress state (Scholz, 1968; Wyss, 1973; Amitrano, 2003; Gulia and Wiemer, 2010), attracting research interest on its spatial and temporal variations.

Generally, analyses of spatial variations of the b value are performed by mapping it on a regularly spaced grid. The inclusion of the earthquakes in the cells can follow different rules (minimum number of events, maximum distance from the centre of the cell, etc.) (Wiemer and Wyss, 1997, 2002) producing, in some cases, overlapping cells or, in other cases, earthquakes that are not included in any cell (Kamer and Hiemer, 2015; Godano et al., 2022). This may prevent a formally correct statistical comparison between different cells of the grid. Some authors weight each earthquake on the basis of its distance from the grid node of interest (Tormann et al., 2014). Many authors have applied this method to several regions of the world (see, among others, Kamer and Hiemer (2015); Taroni et al. (2021); García-Hernández et al. (2021); Pino et al. (2022)). However, it introduces correlations in the grid of the b values. Recently, Godano et al. (2022) introduced a parameter-free method producing fully independent b values and reducing the number of missed earthquakes.

Decreases of b have been proposed to indicate the occurrence of foreshocks before a large earthquake (Papadopoulos, 1988; Papadopoulos et al., 2018, 2010) or to characterize the stress field in a volcanic area (Tramelli et al., 2021). In a recent paper, Gulia and Wiemer (2019) suggested that a smaller b can discriminate between foreshocks and mainshocks in seismic sequences. However, Lombardi (2022) questioned this result because the completeness magnitude m_c (see next paragraph for details on this parameter) could be biased, causing a biased estimation of the b value.

Here, we perform a detailed analysis of the method introduced by Godano et al. (2023) for m_c evaluation in order to verify its reliability, and consequently, the reliability of the connected b value estimations. Then, we apply the method to real-time discrimination of earthquake foreshocks and aftershocks for the Amatrice - Norcia sequence in Italy, following the selection procedure adopted by Gulia and Wiemer (2019) and adopting a blind procedure for the earthquake selection.

2 The evaluation of m_c

The magnitude of completeness, m_c, is defined as the lowest magnitude at which earthquakes are reliably recorded and reported in earthquake catalogues (Rydelek and Sacks, 1989). Its evaluation is extremely important because its underestimation will cause an underestimation of the b value. Conversely, its overestimation implies a loss of information and a bias in the deter-

*Corresponding author: cataldo.godano@unicampania.it

mination of the b value, due to the reduction of magnitude range. Several methods have been proposed for estimating the m_c value (Wiemer and Wyss, 2000; Cao and Gao, 2002; Ohmura and Kawamura, 2007; Godano, 2017; Godano et al., 2023; Godano and Petrillo, 2023; Roberts et al., 2015). In the following list we report and discuss some of the methods that are based on earthquake catalogues, even though there exist other methods (not considered here) that are based on seismic networks (Mignan and Woessner, 2012; Tramelli et al., 2013).

- *The maximum curvature technique* (Wiemer and Wyss, 2000) recognizes m_c as the magnitude at which the Gutenberg-Richter law reaches its maximum value. This method tends to underestimate m_c (Mignan and Woessner, 2012), and consequently, also the b value. Indeed, Wiemer (2001) add 0.2 to their estimated m_c, which is, in some sense, arbitrary.

- *The goodness of fit test* (Wiemer and Wyss, 2000) evaluates the correlation coefficient r of the linearized expression of the Gutenberg-Richter law as a function of a threshold magnitude m_{th}. When r reaches its maximum, or a stable value, then $m_{th} = m_c$. The method presents the disadvantage that the r value for a linearized expression could be, in some cases, unstable, leading to a biased estimation of m_c and b (Mignan and Woessner, 2012).

- *The harmonic mean method* (Godano, 2017) is based on the observation that the harmonic mean of an exponential distribution increases linearly with m_{th}. Consequently, it deviates from linearity for $m_{th} < m_c$. Although the method presents some advantages, similar to the goodness of fit test, the instability of r can produce a biased estimation of m_c and b.

- *The entire magnitude range method* (Ogata and Katsura, 1993) multiplies the Gutenberg-Richter relationship in Eqn. (1) by the cumulative Gaussian distribution of the parameters μ and σ. This implies that at $m = \mu + \sigma$, 50% of the earthquakes are recorded in the catalogue and this probability increases to 95% if $m = \mu + 2\sigma$. The advantage of the method is represented by the possibility of defining a magnitude probability density function for the whole range of magnitudes present in the catalogue. However, above the best completeness value, this method does not describe the gradual curvature of the GR distribution correctly by not multiplying the detection function by the theoretical GR law (Mignan and Woessner, 2012).

- *The b value stability approach* (Cao and Gao, 2002) evaluates the b value as a function of m_{th} and considers $m_{th} = m_c$ when b reaches a stable value. The problem with such a method is the strong fluctuations of the b value at higher m_{th} due to undersampling (Mignan and Woessner, 2012).

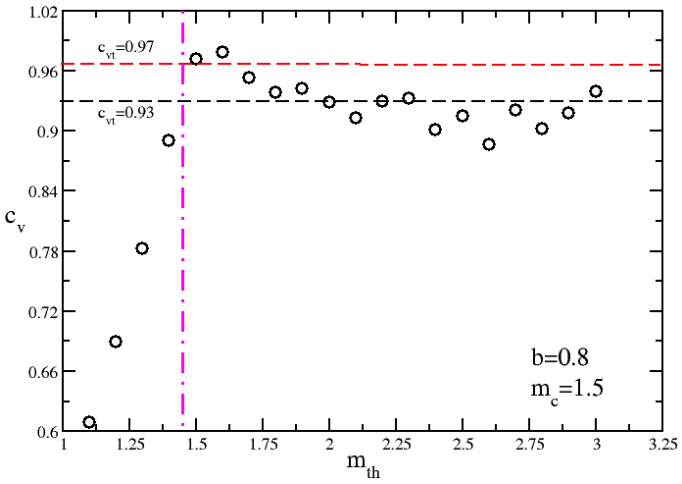

Figure 1 c_v as a function of m_{th} for a simulated catalogue. The dashed lines represent two values of c_{vt}. The vertical dot-dashed magenta line represents point from which we select the best m_{th} The values of b and m_c used to produce the catalogue are also reported in the figure.

2.1 Estimating m_c using the c_v based method.

In the following we will use the method introduced by Godano et al. (2023). The method can be considered a generalization of the one introduced by Cao and Gao (2002) based on b value stabilization. Conversely, Godano et al. (2023) introduce second-order statistics, observing that the variability coefficient (defined as the ratio between the standard deviation and the average value) of an exponential distribution assumes a value equal to 1. More precisely, we define the quantity $m_1 = m - m_{th}$ and evaluate its variability coefficient

$$c_v = \frac{\sigma_{th}}{\langle m_1 \rangle} \tag{2}$$

with σ_{th} being the standard deviation of m_1 and $\langle m_1 \rangle$ its average value. m_1 must follow an exponential distribution whose c_v assumes the value 1. As a consequence, when evaluating c_v as a function of a threshold magnitude m_{th}, c_v assumes a value $\simeq 1$ at $m_{th} = m_c$, where the distribution becomes a purely exponential distribution. An example for a simulated catalogue (see next paragraph for details) is shown in Fig. 1. As can be seen, c_v does not assume the value of 1, typical of a purely exponential distribution, for all the m_{th} values. This occurs because of the fluctuation of the distribution around the purely exponential one. In other cases (not shown here), c_v can assume values slightly larger than 1. For this reason, it is opportune to introduce a c_v threshold value (let us call it c_{vt}) above which the distribution can be considered a purely exponential distribution. More precisely, we choose m_c to be the smallest m_{th} where c_v is larger than the threshold c_{vt}. Here we show, as an example, two values of c_{vt}: 0.93 and 0.97. In both cases the m_c value is correctly identified for the example shown here. A more accurate investigation of the appropriate c_{vt} value is performed below.

Let us test the reliability of the method by means of some simulations.

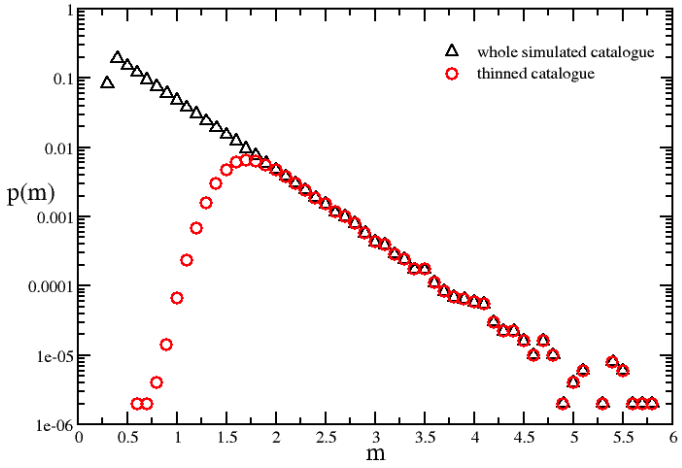

Figure 2 An example of the GR distribution for a simulated catalogue before and after thinning.

2.2 Randomly simulated catalogues

In order to test the reliability of the method, we simulated 10^5 catalogues with 20000 earthquakes and a b value randomly chosen from a uniform distribution in the range of [0.5,1.5]. Then, each catalogue is thinned using the Ogata and Katsura (1993) approach. The method consists of multiplying the Gutenberg-Richter distribution by an $erfc(m)$ function. This provides the number of events to be removed from the catalogue for each $m < m_c$. While simulated catalogues can be truncated at a given threshold magnitude, this does not correctly simulate experimental catalogues containing some, though not all, events with $m < m_c$. The $erfc(m)$ parameters have been selected on the basis of the following rules: μ has been randomly generated in the range [1.5,2.5], whereas σ is fixed at 0.1 considering $m_c = \mu + 2\sigma$. An example of the GR distribution for a simulated catalogue, before and after thinning, is shown in Fig. 2. Then, for each catalogue, we estimate m_c using the Godano et al. (2023) method and b by means of the standard maximum likelihood method (Aki, 1965) and evaluate the quantities $\Delta b = b - b_e$ and $\Delta m_c = m_c - m_{c_e}$, where b and m_c are the parameters used for the simulation and b_e and m_{c_e} are the corresponding estimated values. The distributions of Δb and Δm_c are then evaluated.

There are three quantities affecting Δb and Δm_c, namely N, the minimum number of events in the range $m_{max} - m_c$, the range itself $\Delta m = m_{max} - m_c$, and c_{vt}. More precisely, we evaluate the distributions of Δb and Δm_c using only catalogues:

1. with a number n of events with $m \geq m_c$ larger than or equal to a given value of N without any restriction on Δm and using c_{vt}=0.97
2. with Δm larger than a given value without any restriction on N and using c_{vt}=0.97
3. with different values of c_{vt} without any restriction on Δm and $N = 100$ (this restriction is adopted to evaluate a reliable value of σ_{th})

The evaluated distributions are reported in Figures 3 to 5. In all cases the distributions are sharply peaked (indicating supergaussian distributions) at $\Delta b = 0$ and at $\Delta m_c \simeq -0.25$, revealing a small tendency to overestimate m_c. In the supplementary information we report the results of the Kolmogorov-Smirnov test at a 99% confidence level (test statistic$= 0.31$) in order to reject the hypothesis that the samples follow a Gaussian distribution. The results are not strongly influenced by N and Δm, although for $N = 300$ and $\Delta m = 3$ long tails in Δb distributions are avoided. However, for these values more than 50% of the catalogues are discarded due to a small number of events or too small a magnitude range.

The overestimation of m_c when c_{vt}=0.97 suggests that this parameter also influences our results. As a consequence we perform a sensitivity analysis, varying c_{vt} in the range [0.93,0.99]. Fig. 5 reveals that $p(\Delta m_c)$ is correctly peaked at $\Delta m_c = 0$ when c_{vt}=0.93, which can be assumed as the best value for c_{vt}.

2.3 Epidemic Type Aftershock Sequence (ETAS) simulated catalogues

The ETAS model represents the gold standard for testing seismic clustering hypotheses and forecasting (Ogata, 1988, 1998; Helmstetter and Sornette, 2003; Console et al., 2007; Lombardi and Marzocchi, 2010; Zhuang, 2011, 2012). In this model the occurrence rate λ of an event with magnitude $m > m_0$, at a position (x, y) and a time t, can be written as

$$\lambda(x,y,t|\mathcal{H}_t) = \mu(x,y) + \sum_{j:t_j<t} K10^{\alpha(m_j-m_0)} \frac{(p-1)c^{p-1}}{(t-t_j+c)^p} \frac{q-1}{\pi} (\delta(m_j))^{q-1} [(x-x_j)^2 + (y-y_j)^2 + \delta(m_j)]^{-q} \quad (3)$$

where the sum extends over all previous events that occurred in a certain region, $\mu(x, y)$ describes the time-stationary background rate, $\delta(m) = d10^{\gamma m}$ from Kagan (2002) and the set $\hat{\theta} = (p, \alpha, c, K, d, q, \gamma)$ contains the fitting parameters of the model. The estimation of the set $\hat{\theta}$ that best fits the experimental data can be performed using maximum likelihood methods (Lippiello et al., 2014; Ogata, 1998; Y., 1983; Ogata and Zhuang, 2006) or different types of tuning techniques (Petrillo and Lippiello, 2020, 2023).

The generation of an ETAS catalog is a standard procedure described in Zhuang et al. (2004); Zhuang and Touati (2015) and de Arcangelis L. et al. (2016). The first step is setting the background seismicity $\mu(x, y)$. This represents the zeroth order generation in a self-exciting branching process and a certain number n_0 of events are created. Each of these elements generate a certain number of offspring, i.e, the aftershocks. The number n_1, the occurrence, and the spatiotemporal position of the aftershocks depend on the functional form $\lambda(x, y, t)$ and on the parameters $\hat{\theta}$. In practice, the number of aftershocks is extracted from a Poisson distribution with an average dictated by the productivity law. For each offspring, the occurrence time is extracted based on the Omori-Utsu law and the location is based on the spatial

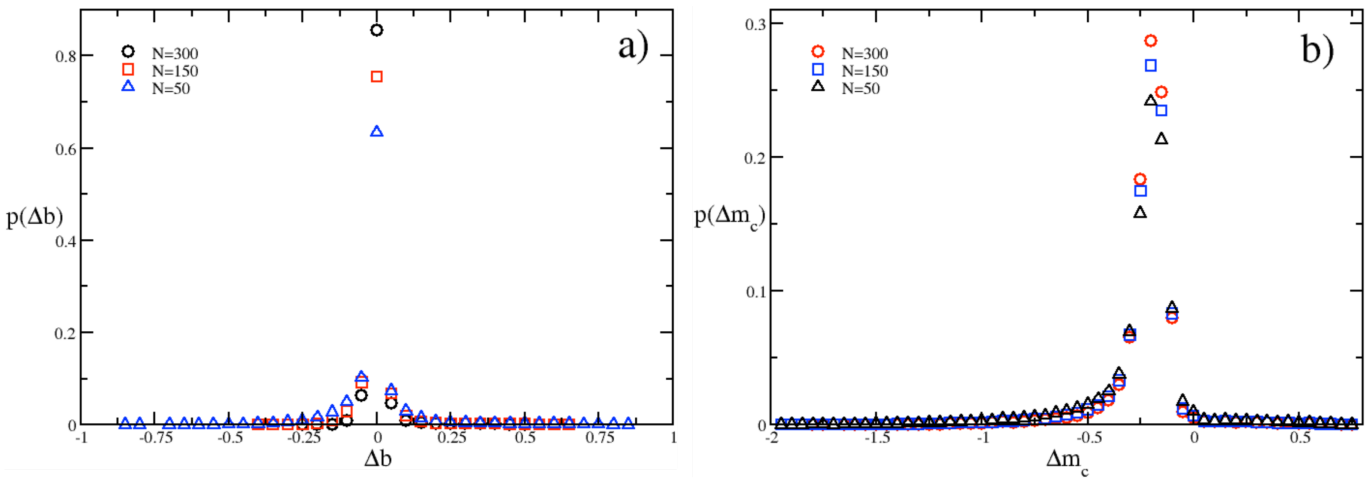

Figure 3 Distributions of Δb (panel (a)) and Δm_c (panel (b)) for different values of N and c_{vt}=0.97.

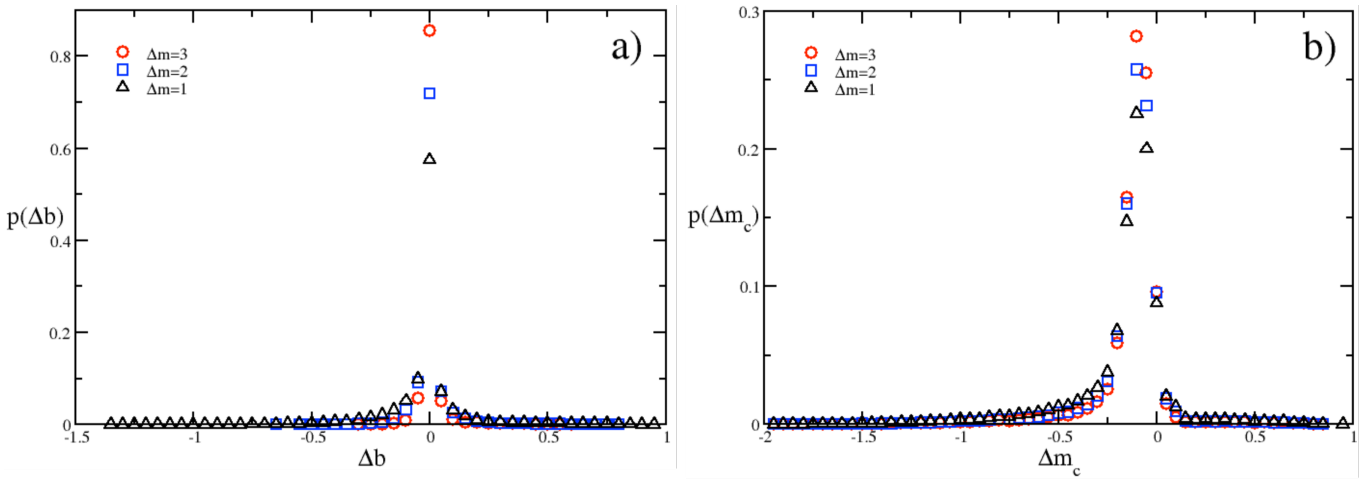

Figure 4 The distributions of Δb (panel (a)) and Δm_c (panel (b)) for different values of Δm and c_{vt}=0.97.

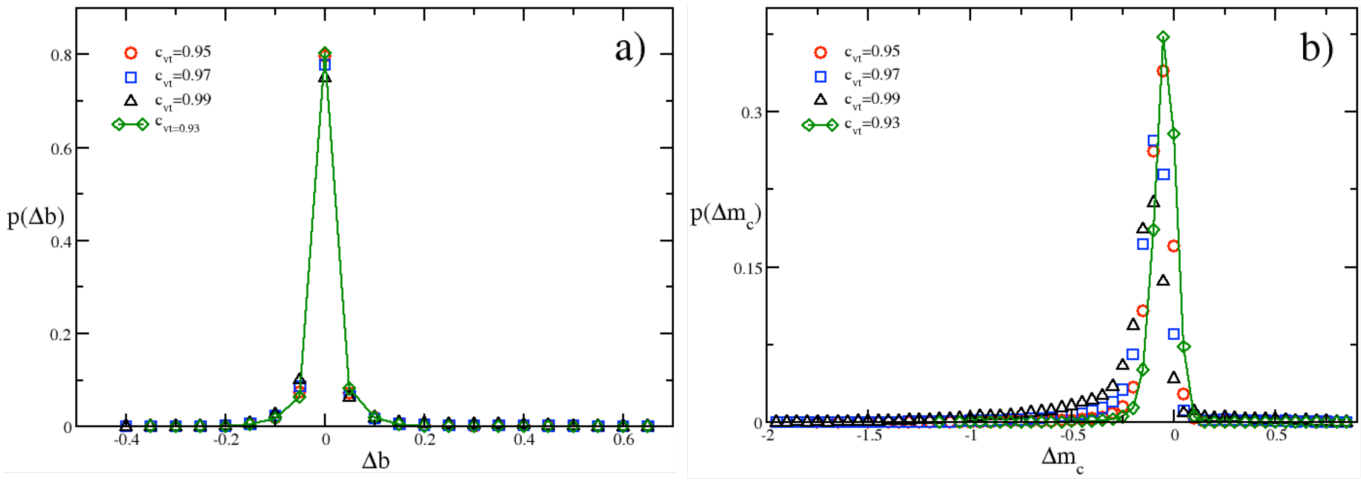

Figure 5 The distributions of Δb and Δm_c for different values of c_{vt}. Here N and Δm are fixed at 100 and 2 respectively.

distribution. As a last step, the magnitude of the event is assigned obtaining the value from the Gutenberg-Richter law in Eqn. (1), since we are assuming magnitude independence among triggered events (Petrillo and Zhuang, 2022, 2023). This is the first-order generation of events. The previous step is repeated considering $n_j = n_{j-1}$ and it is iterated until $n_{j*} = 0$. We would like to emphasize that the numerical catalogs generated using this method do not exclude any events; in other words, no completeness threshold is used to get the simulation. In this study we employ the parameters optimized by Petrillo and Lippiello (2023). In order to verify the reliability of the method in analyzing time variations of the b value we simulated 5 ETAS (Ogata, 1999) catalogues with about 10^6 events and different values of b, in particular $b = 0.6, 0.8, 1.0, 1.2, 1.4$. Then, employ-

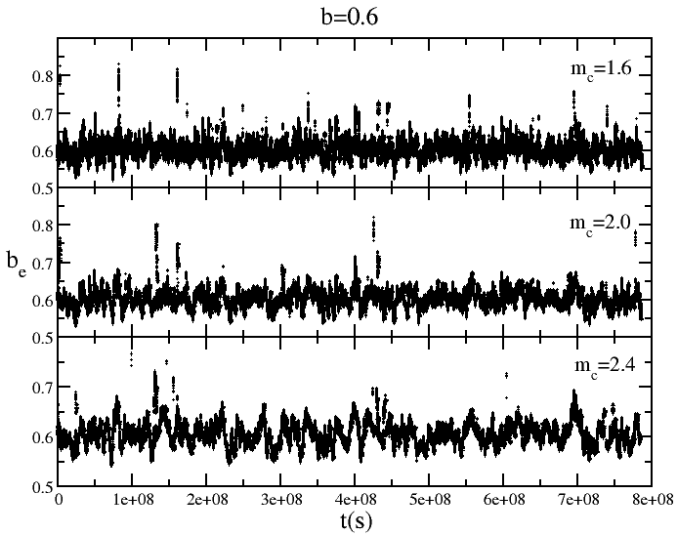

Figure 6 The time variation of the b_e value for the catalogue with b=0.6 thinned at three different m_c values.

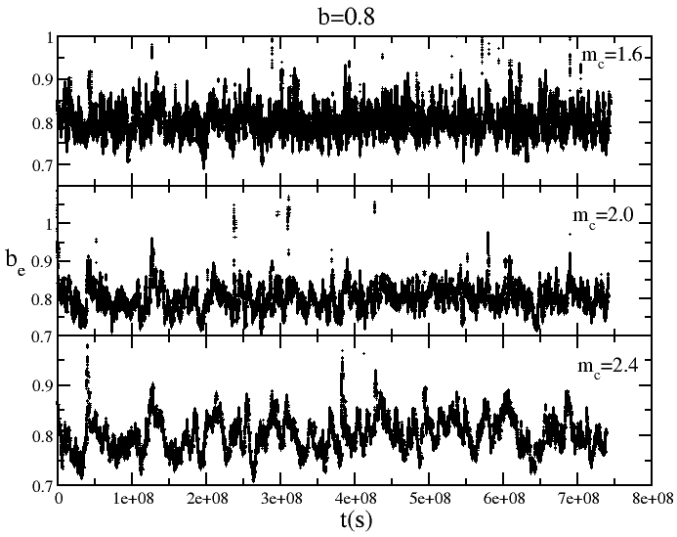

Figure 7 The time variation of the b_e value for the catalogue with b=0.8 thinned at three different m_c values.

ing the same thinning procedure used before, for each value of b we obtain 3 different incomplete catalogues by setting $m_c = 1.6, 2.0$, and 2.4, for a total of 15 synthetic incomplete catalogues. The temporal variations of the b value are finally obtained by considering windows of 1000 events, sliding on one event at a time. For each window we evaluate m_c with the Godano et al. (2023) method and b by maximizing the likelihood (Aki, 1965). In this case we use $N = 150$, Δm = 2 and $c_{vt} = 0.93$. Of course, we expect no time variation of the b and m_c values or, at least, weak fluctuations of their values around the 'true' values. However Figures 6 - 10 show that b appears to fluctuate around an underestimated value. In general, the changes in the b value could reflect the physical processes of stress evolution and crack growth. However, the fluctuations observed in the analyses are within statistical error, so in this case, a decrease in b is not an indication of precursor phenomena. For high values of the magnitude of completeness, some gaps are present in $b_e(t)$. This is explained by the fact that in data

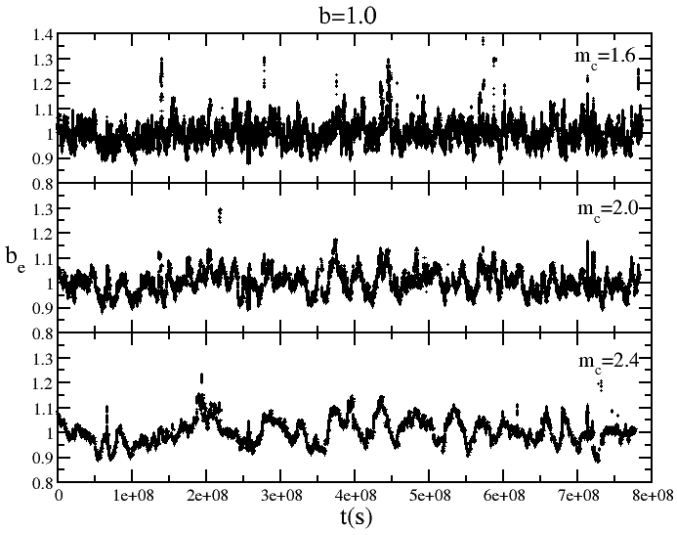

Figure 8 The time variation of the b_e value for the catalogue with b=1.0 thinned at three different m_c values.

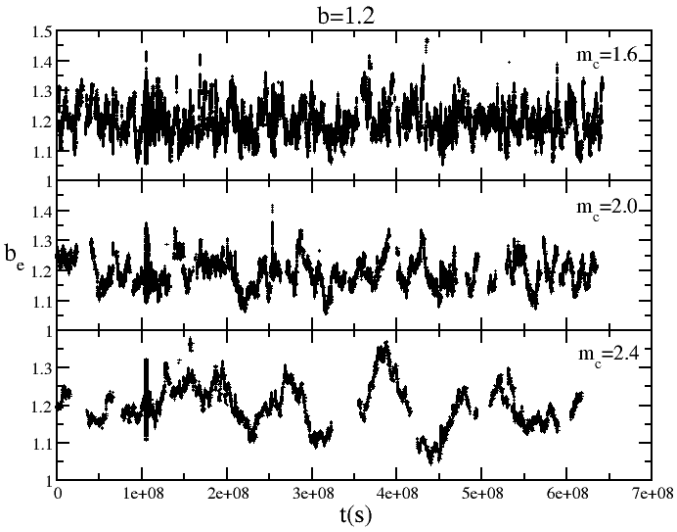

Figure 9 The time variation of the b_e value for the catalogue with b=1.2 thinned at three different m_c values.

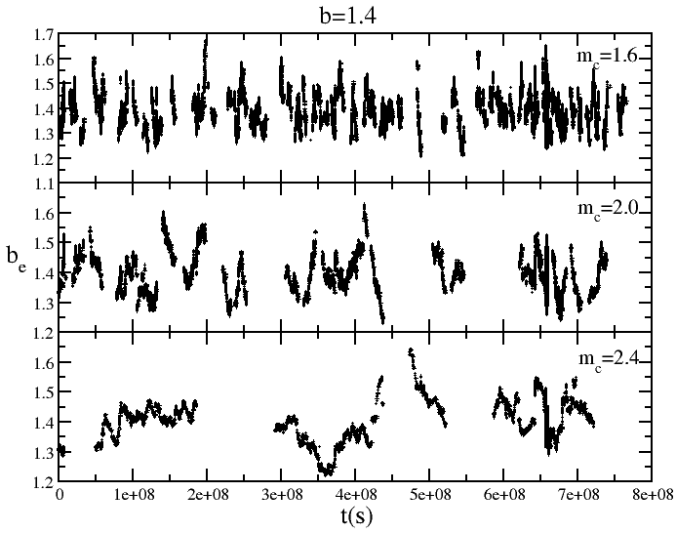

Figure 10 The time variation of the b_e value for the catalogue with b=1.4 thinned at three different m_c values.

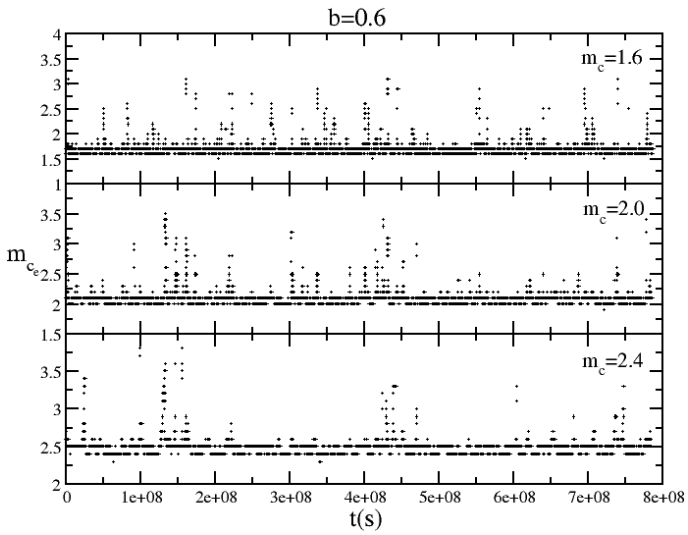

Figure 11 The time variation of the m_{c_e} value for the catalogue with b=0.6 thinned at three different m_c values.

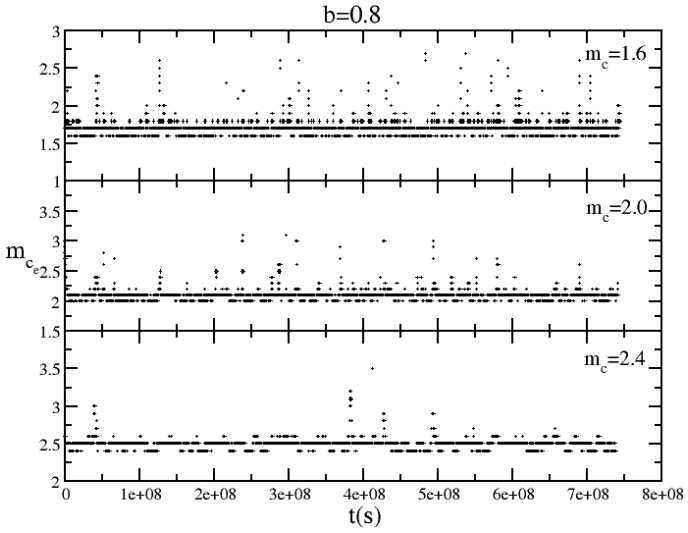

Figure 12 The time variation of the m_{c_e} value for the catalogue with b=0.8 thinned at three different m_c values.

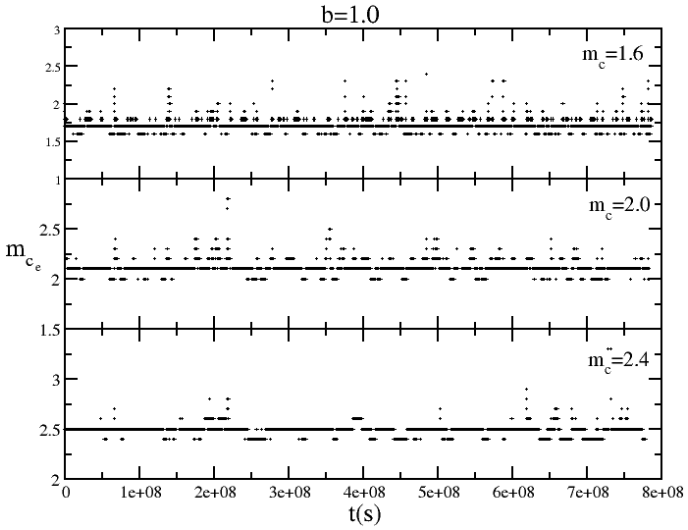

Figure 13 The time variation of the m_{c_e} value for the catalogue with b=1.0, thinned at three different m_c values.

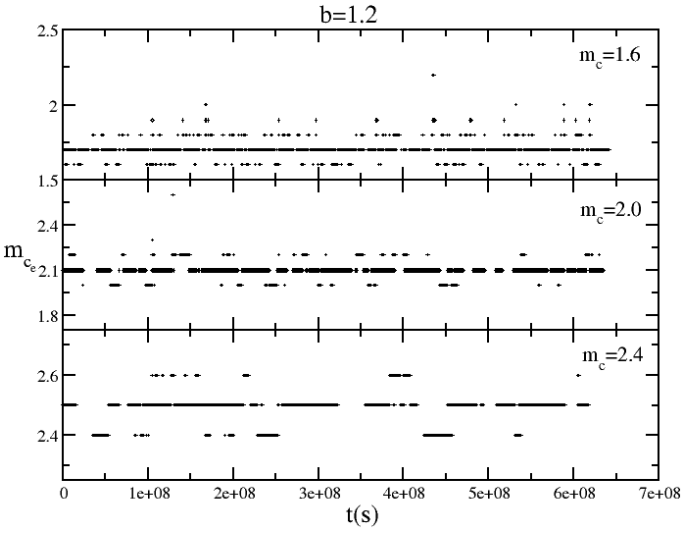

Figure 14 The time variation of the m_{c_e} value for the catalogue with b=1.2, thinned at three different m_c values.

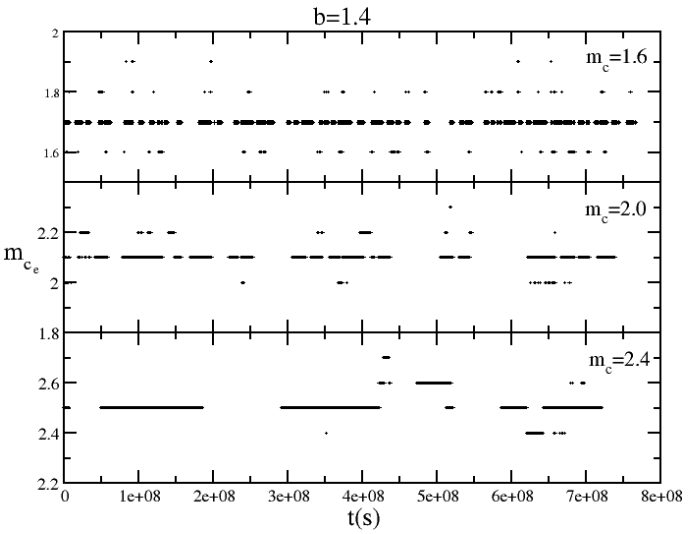

Figure 15 The time variation of the m_{c_e} value for the catalogue with b=1.4, thinned at three different m_c values.

that do not fall within the constraints of the evaluation of b_e, in particular, the required number of events N is greater than the number of events recorded in the catalogue.

Figs. 11 - 15 show the estimation of m_c for the same thinned catalogues. m_c estimates appear to be stable but are overestimated by a very small quantity, for each value of simulated b and completeness magnitude m_c. The error bars for b_e and m_{c_e} are not shown in order to make the graphs clearer. Furthermore, as this is a test on synthetic catalogues, there is no intention to evaluate the changes in b for forecasting purposes, but only to assess the used estimation method.

Fig. 16 shows the distribution of the b_e values for the different catalogues generated with the different b, confirming the tendency to underestimate b independently of the m_c value.

For comparison we evaluate the b values using the maximum curvature method for estimating m_c. Fig. 17 reveals that b_e significantly differs from the 'true' value

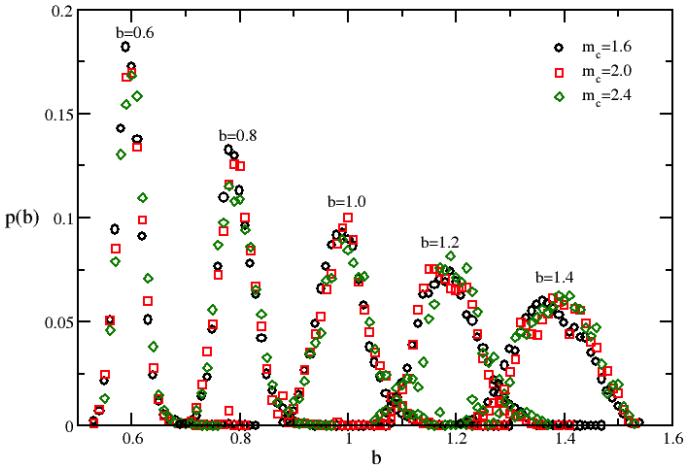

Figure 16 The distributions of the b_e value for the different catalogues thinned at the different m_c values.

in the case of b=1.0 and worsen as m_c increases. Indeed, the distribution's peak is large for m_c=1.6, bimodal for m_c=2.0, and sharply peaked at b_e=0.76 for m_c=2.4. Very similar behaviour is observed, but not reported here, for the other values of b.

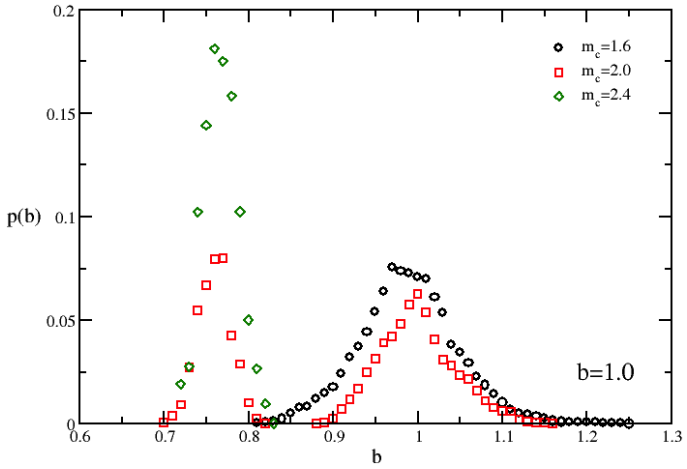

Figure 17 The distributions of the b_e in the case of b=1.0 and for the different m_c values, when m_c is estimated with the maximum curvature method.

3 Verifying the real-time discrimination of earthquake foreshocks and aftershocks

Analyzing the Amatrice-Norcia and Kumamoto sequences, Gulia and Wiemer (2019) demonstrated that variations in b can act as a discriminant between foreshocks and aftershocks. In practice, for the Italian Amatrice-Norcia sequence, they measured a reference value, b_r, for the background, considering the 4 years preceding the target earthquake $\mathcal{E}$. Then, removing events during the first 3 days after $\mathcal{E}$ because of short term aftershock incompleteness, they computed $\Delta b = b_{\mathcal{E}} - b_r$, where $b_{\mathcal{E}}$ is the b value computed using earthquakes ocurring after the event $\mathcal{E}$. The completeness magnitude m_c was estimated through the maximum-curvature method and the b value using a maximum-likelihood estimation on a sample of $N = 250$ events (consequently, the time series $b(t)$ was obtained with an element-wise moving window). Finally, b_r was extracted by calculating the median of all $b(t)$. The calculation of $b_{\mathcal{E}}$ follows the same rules but, because aftershock sequences are data-rich, the study used $N = 400$. However, Gulia and Wiemer (2019) also tested the results for slightly different values of N, and verified the robustness of their results.

3.1 Applying the c_v method - the comparison

Some authors questioned the results of Gulia and Wiemer (2019), arguing that fluctuations in the b value may not be a dependable indicator of stress in these instances. Instead, they could be attributed to a mixture of inconsistencies in the data and inefficiencies in estimation methods (Lombardi, 2022). Moreover, van der Elst (2021) confirms the findings of Gulia and Wiemer (2019), although at a reduced level. For this reason, to try to reduce estimation bias, we apply the Godano et al. (2023) method to the catalogue selected by Gulia and Wiemer (2019). More precisely, we evaluate m_c (using the Godano et al. (2023) method with a $c_{vt} = 0.93$) and b in the same windows of $N = 250$ events, sliding by one event at time and discarding all the windows with a number of events with $m \geq m_c$, larger than 50 and fulfilling the condition $m_{max} - m_c > 2$. Even if these conditions lead to discarding a large number of windows, the result of Gulia and Wiemer (2019) is confirmed. Indeed, both the average $\langle b \rangle$ value and its median b_M, before the occurrence of the Amatrice earthquake, are larger than the same values calculated after its occurrence and before the occurrence of the Norcia earthquake (Fig. 18). Interestingly, the difference between $\langle b \rangle$ and b_M, before the occurrence of the Amatrice earthquake, is large, revealing a significant skewness of the b distribution. Conversely, after the occurrence of the Amatrice earthquake, $\langle b \rangle - b_M$ assumes a very small value, indicating a Gaussian-like b value distribution.

Fig. 19 shows an example of two Gutenberg-Richter (GR) distributions for two different time windows (randomly chosen) before and after the Amatrice earthquake occurrence.

3.2 A blind algorithm

We now test an automatic algorithm for the real-time discrimination of earthquake foreshocks and aftershocks on the Italian catalogue available at the web-site http://terremoti.ingv.it/. We adopted the following algorithm:

1. Identify all the earthquakes with magnitude $m \geq 5.5$ (let us call them mainshocks);
2. For each one of them, we evaluate the aftershock radius following the Utsu and Seki (1954) formula $r = 0.05 \times 10^{0.5m} km$;
3. Identify all the events with a distance d smaller than r in the 4 years preceding the occurrence of the mainshock;

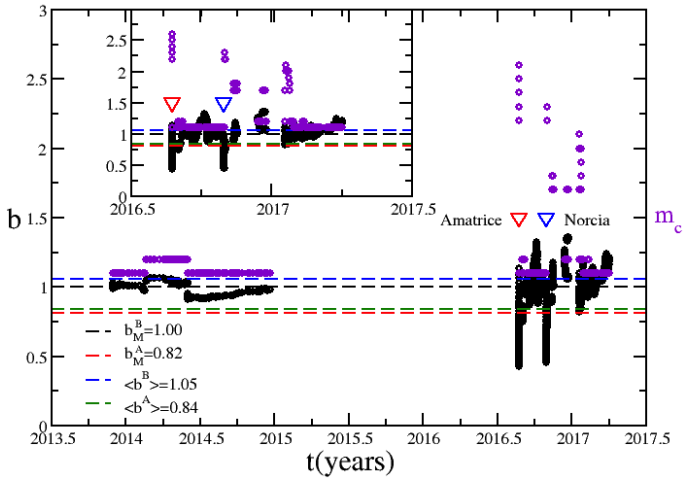

Figure 18 The b values (black circles) versus time. The dashed lines represent $\langle b \rangle$ and b_M (see legends for details) computed before (B) and after (A) the occurrence of Amatrice earthquake. The violet circles represent the m_c values. The triangles indicate the occurrence of the Amatrice and Norcia earthquakes. (Inset) Zoom of the main panel performed between 2016.5 and 2017.5.

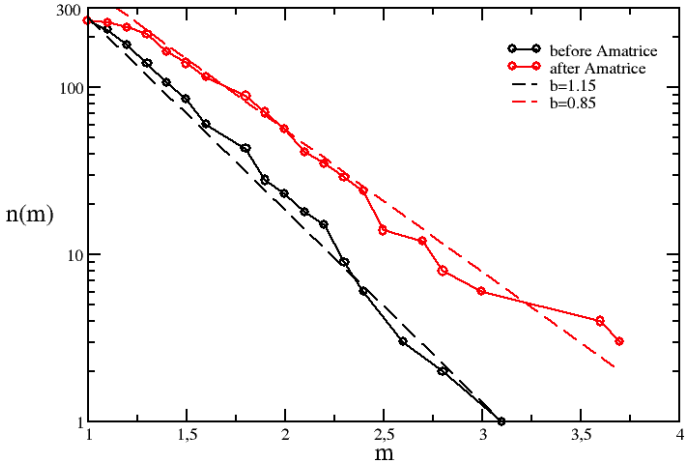

Figure 19 The Gutenberg-Richter distributions 4 years before and 1 year after the Amatrice earthquake occurrence. The dashed lines represent the fitted GR laws.

4. If the number n_b of events preceding the mainshock is smaller than 500 we double the value of r;

5. Identify all the events with a distance d smaller than r in 1 year following the occurrence of the mainshock;

6. We remove short-term aftershock incompleteness by means of the Helmstetter et al. (2006) method using the parameters optimized for Italy in Petrillo and Lippiello (2020);

7. If the number n_a of events following the mainshock is smaller than 500 we discard the mainshock from the analysis;

8. We evaluate the b and m_c values as a function of time following the previously described method.

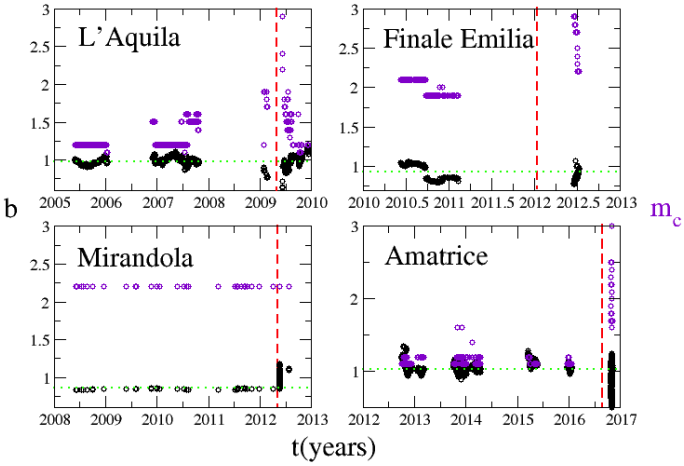

Figure 20 $b(t)$ and $m_c(t)$ for four of the mainshocks analysed here. Vertical red dashed lines represent the occurrence time of each mainshock. Horizontal green dotted lines represent the pre-event average b-value.

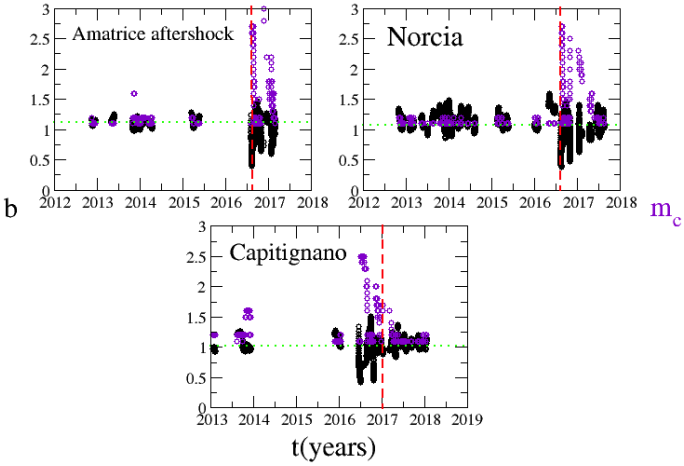

Figure 21 The $b(t)$ and $m_c(t)$ for the other three mainshocks analysed here. Vertical red dashed lines represent the occurrence time of each mainshock. Horizontal green dotted lines represent the pre-event average b-value.

On the basis of this algorithm, we identified mainshocks in the Italian catalogue. Item 3 has been applied only one time for the Finale Emilia earthquake. We discarded two mainshocks because n_a assumed values smaller than 500 for them. Both of these mainshocks ($m = 5.8$ and $m = 5.9$) occurred in the Aeolian Arc at a depth larger than 144 km. As a consequence, 7 earthquakes remain in the analysis: L'Aquila ($m = 6.1$), Finale Emilia ($m = 5.8$), Mirandola ($m = 5.6$), Amatrice ($m = 6.0$), an Amatrice aftershock ($m = 5.9$), Norcia ($m = 6.5$) and Capitignano ($m = 5.5$) close to L'Aquila. The information about the location, the magnitude, and the occurrence time of the mainshocks considered in the blind test is listed in Table 1.

An important deviation from Gulia and Wiemer (2019) is the use of the $M5.5 - 5.9$ earthquakes. This addition was decided in order to introduce more events in the blind test. A second deviation from Gulia and Wiemer (2019) is the use of the Utsu and Seki (1954) formula to identify the aftershocks and the background activity within a circular radius. This choice represents

Earthquake	Date	Location	Magnitude
L'Aquila	6 April 2009	42.42, 13.39	6.1
Finale Emilia	20 May 2012	44.80, 11.19	5.8
Mirandola	20 May 2012	44.85, 11.06	5.6
Amatrice	24 August 2016	42.70, 13.22	6.0
Amatrice aftershock	26 October 2016	42.90, 13.09	5.9
Norcia	30 October 2016	42.84, 13.11	6.5
Capitignano	18 January 2017	42.48, 13.28	5.5

Table 1 List of the mainshocks considered in the blind test including coordinates, occurrence time and magnitude.

the simplest one that can be performed in a blind algorithm, as it does not require the knowledge of the focal mechanism, the identification of the fault plane and its extension, and the localization of the mainshock on the fault. Moreover, the epicentral map (see supplementary information) of the chosen earthquakes reveals that, concerning the aftershocks, their selection corresponds to on-fault seismicity. Conversely, the selected background seismicity includes off-fault events. However, this does not represent a large difference with the Gulia and Wiemer (2019) method. Indeed, Gulia and Wiemer (2019) had to enlarge the investigated area in order to include a number of events sufficient to constrain the b_r value. The $b(t)$ and $m_c(t)$ values are shown in Figs. 20 and 21, and $\langle b \rangle$, b_M, and the b standard deviation σ_b before and after the occurrence of the 7 mainshocks are reported in Table 2.

Earthquake	before			after		
	$\langle b \rangle$	b_M	σ_b	$\langle b \rangle$	b_M	σ_b
L'Aquila	0.98	0.98	0.058	0.96	0.97	0.085
Finale Emilia	0.93	1.0	0.095	0.84	0.8	0.19
Mirandola	0.86	0.88	0.1	1.14	1.15	0.016
Amatrice aftershock	1.06	1.06	0.074	1.02	1.04	0.14
Amatrice	1.03	1.06	0.15	0.93	0.9	0.13
Norcia	1.07	1.06	0.16	1.0	1.02	0.092
Capitignano	1.02	1.03	0.16	1.07	1.07	0.087

Table 2 $\langle b \rangle$, b_M and σ_b for the 7 mainshocks analysed here, before and after their occurrence.

Earthquake	before			after		
	$\langle b \rangle$	b_M	σ_b	$\langle b \rangle$	b_M	σ_b
L'Aquila	0.99	0.99	0.064	0.95	0.96	0.082
Finale Emilia	0.93	1.0	0.094	0.86	0.85	0.062
Amatrice aftershock	1.11	1.10	0.057	0.94	0.94	0.14
Amatrice	1.02	1.04	0.16	1.02	1.05	0.16
Norcia	1.03	1.04	0.18	0.90	0.92	0.13
Capitignano	1.02	1.03	0.16	1.09	1.1	0.096

Table 3 $\langle b \rangle$, b_M and σ_b for the 6 mainshocks analysed considering restricted time period before (2 years) and after (0.5 years) the target mainshock.

Moreover, in order to test the robustness of the time parameters considered in the blind test, we show in Table 3 that halving the time period before and after the occurrence of the mainshock target does not change the results substantially. Note that halving the time period for the Mirandola earthquake is excluded from the analysis because the number of aftershocks is smaller than 500.

A t-test reveals that the b values before and after the occurrence of the mainshocks cannot be considered different at a 95% significance level. This implies that the discrimination between foreshocks and aftershocks cannot be performed using a blind algorithm.

Conclusions

We extensively tested the method proposed by Godano et al. (2023) for evaluating the completeness magnitude (m_c), which we referred to as the c_v method. The testing involved randomly generated catalogues with varying values of b and m_c, as well as simulated catalogues generated using ETAS models with fixed b and m_c values. In all cases, the method exhibited excellent performance. The distributions of the estimated values compared to the "true" values showed a supergaussian shape, centered around zero. Using the c_v method we then tested the results of Gulia and Wiemer (2019) for the Amatrice-Norcia earthquake sequence, confirming their results when using their catalogue, which represents a specific selection of the Italian catalogue. The use of a more reliable method in the estimation of m_c and b represents a stronger confirmation of their results, resolving doubts about possible biases introduced by an underestimation of m_c (Lombardi, 2022). However, when applying a blind algorithm to the Italian catalogue, no differences were found in the b values before and after the occurrence of the mainshock. This result indicates that: 1) the difference in b values is significant when an appropriate catalogue selection is made, supporting the notion that the b value serves as a reliable stress indicator. Specifically, if a genuine mainshock is imminent, the stress increases while the b value decreases; 2) the decrease in the b value cannot be detected using our blind approach and, consequently, cannot be utilized for real-time predictive purposes. Of course, other blind approaches could, conversely, confirm the Gulia and Wiemer (2019) results.

Acknowledgements

This study has been supported by the PRIN PNRR DIRECTIONS Project, No P20229KB4F, funded by the Italian Ministry of Education and Research. The authors thank two anonymous reviewers for their comments on this study.

Data and code availability

The catalogue used in this work can be downloaded at the web-site http://terremoti.ingv.it/.

Competing interests

The authors have no competing interests.

References

Aki, K. Maximum likelihood estimate of b in the formula $\log N = a - bM$ and its confidence limits. *Bull. Earthq. Res. Inst., Univ. Tokyo*, 43:237–239, 1965.

Amitrano, D. Brittle-ductile transition and associated seismicity: Experimental and numerical studies and relationship with the b value. *Journal of Geophysical Research: Solid Earth*, 108(B1): 2044, 2003. doi: 10.1029/2001JB000680.

Cao, A. and Gao, S. S. Temporal variation of seismic b-values beneath northeastern Japan island arc. *Geophysical Research Letters*, 29(9):48–1–48–3, 2002. doi: https://doi.org/10.1029/2001GL013775.

Console, R., Jackson, D., and Kagan, Y. Using the ETAS Model for Catalog Declustering and Seismic Background Assessment. *Pure and Applied Geophysics*, 167:819–830, 2007. doi: 10.1007/s00024-010-0065-5.

de Arcangelis L., Godano, C., R., G. J., and E., L. Statistical physics approach to earthquake occurrence and forecasting. *Physics Reports*, 628:1–91, 2016. doi: 10.1016/j.physrep.2016.03.002.

García-Hernández, R., D'Auria, L., Barrancos, J., Padilla, G. D., and Pérez, N. M. Multiscale Temporal and Spatial Estimation of the b-Value. *Seismological Research Letters*, XX:1–13, 2021. doi: https://doi.org/10.1785/0220200388.

Godano, C. A new method for the estimation of the completeness magnitude. *Physics of the Earth and Planetary Interiors*, 263:7 – 11, 2017. doi: https://doi.org/10.1016/j.pepi.2016.12.003.

Godano, C. and Petrillo, G. Estimating the Completeness Magnitude mc and the b-Values in a Snap. *Earth and Space Science*, 10(2), 2023. doi: 10.1029/2022EA002540.

Godano, C., Convertito, V., Pino, N. A., and Tramelli, A. An Automated Method for Mapping Independent Spatial b Values. *Earth and Space Science*, 9(6):e2021EA002205, 2022. doi: https://doi.org/10.1029/2021EA002205.

Godano, C., Petrillo, G., and Lippiello, E. Evaluating the incompleteness magnitude using an unbiased estimate of the b value. *Geophysical Journal International*, submitted, 2023.

Gulia, L. and Wiemer, S. The influence of tectonic regimes on the earthquake size distribution: A case study for Italy. *Geophysical Research Letters*, 37(10), 2010. doi: 10.1029/2010GL043066.

Gulia, L. and Wiemer, S. Real-time discrimination of earthquake foreshocks and aftershocks. *Nature*, 574:193–199, 2019. doi: 10.1038/s41586-019-1606-4.

Gutenberg, B. and Richter, C. Frequency of earthquakes in California. *Bulletin of the Seismological Society of America*, 34(4): 185–188, 1944.

Helmstetter, A. and Sornette, D. Foreshocks explained by cascades of triggered seismicity. *Journal of Geophysical Research: Solid Earth*, 108(B10):2457, 2003. doi: 10.1029/2003JB002409.

Helmstetter, A., Kagan, Y. Y., and Jackson, D. D. Comparison of Short-Term and Time-Independent Earthquake Forecast Models for Southern California. *Bulletin of the Seismological Society of America*, 96(1):90–106, 2006. doi: 10.1785/0120050067.

Kagan, Y. Y. Aftershock zone scaling. *Bulletin of the Seismological Society of America*, 92(2):641–655, 2002. doi: 10.1785/0120010172.

Kamer, Y. and Hiemer, S. Data-driven spatial b value estimation with applications to California seismicity: To b or not to b. *Journal of Geophysical Research: Solid Earth*, 120(7):5191–5214, 2015. doi: https://doi.org/10.1002/2014JB011510.

Lippiello, E., Giacco, F., Arcangelis, L. d., Marzocchi, W., and Godano, C. Parameter estimation in the ETAS model: Approximations and novel methods. *Bulletin of the Seismological Society of America*, 104(2):985–994, 2014. doi: 10.1785/0120130148.

Lombardi, A. M. Anomalies and transient variations of b-value in Italy during the major earthquake sequences: what truth is there to this? *Geophysical Journal International*, 232(3): 1545–1555, 10 2022. doi: 10.1093/gji/ggac403.

Lombardi, M. and Marzocchi, W. The ETAS model for daily forecasting of Italian seismicity in the CSEP experiment. *Annals of Geophysics*, 53, 2010. doi: 10.4401/ag-4848.

Mignan, A. and Woessner, J. Estimating the magnitude of completeness for earthquake catalogs. *Community Online Resource for Statistical Seismicity Analysis*, 2012. doi: 10.5078/corssa-00180805.

Ogata, Y. Statistical Models for Earthquake Occurrences and Residual Analysis for Point Processes. *J. Am. Stat. Assoc.*, 83(401): 9–27, 1988. doi: 10.2307/2288914.

Ogata, Y. Space-time point-process models for earthquake occurrences. *Annals of the Institute of Statistical Mathematics*, 50(2): 379–402, 1998. doi: 10.1023/A:1003403601725.

Ogata, Y. Seismicity Analysis through Point-process Modeling: A Review. *pure and applied geophysics*, 155(2-4):471–507, 1999. doi: 10.1007/s000240050275.

Ogata, Y. and Katsura, K. Analysis of temporal and spatial heterogeneity of magnitude frequency distribution inferred from earthquake catalogues. *Geophysical Journal International*, 113 (3):727–738, 1993. doi: 10.1111/j.1365-246X.1993.tb04663.x.

Ogata, Y. and Zhuang, J. Space–time ETAS models and an improved extension. *Tectonophysics*, 413(1–2):13 – 23, 2006. doi: http://dx.doi.org/10.1016/j.tecto.2005.10.016.

Ohmura, A. and Kawamura, H. Rate- and state-dependent friction law and statistical properties of earthquakes. *EPL (Europhysics Letters)*, 77(6):69001, 2007. doi: 10.1209/0295-5075/77/69001.

Papadopoulos, G., Minadakis, G., and Orfanogiannaki, K. *Short-Term Foreshocks and Earthquake Prediction*, chapter 8, pages 125–147. American Geophysical Union (AGU), 2018. doi: https://doi.org/10.1002/9781119156949.ch8.

Papadopoulos, G. A. Long-term accelerating foreshock activity may indicate the occurrence time of a strong shock in the Western Hellenic Arc. *Tectonophysics*, 152(3–4):179 – 192, 1988. doi: http://dx.doi.org/10.1016/0040-1951(88)90044-3.

Papadopoulos, G. A., Charalampakis, M., Fokaefs, A., and Minadakis, G. Strong foreshock signal preceding the L'Aquila (Italy) earthquake (M_w 6.3) of 6 April 2009. *Natural Hazards and Earth System Science*, 10(1):19–24, 2010. doi: 10.5194/nhess-10-19-2010.

Petrillo, G. and Lippiello, E. Testing of the foreshock hypothesis within an epidemic like description of seismicity. *Geophysical Journal International*, 225(2):1236–1257, 12 2020. doi: 10.1093/gji/ggaa611.

Petrillo, G. and Lippiello, E. Incorporating Foreshocks in an Epidemic-like Description of Seismic Occurrence in Italy. *Applied Sciences*, 13(8), 2023. doi: 10.3390/app13084891.

Petrillo, G. and Zhuang, J. The debate on the earthquake magnitude correlations: A meta-analysis. *Scientific reports*, 12(1): 20683, 2022. doi: 10.1038/s41598-022-25276-1.

Petrillo, G. and Zhuang, J. Verifying the magnitude dependence in earthquake occurrence. *Physical Review Letters*, 131(15): 154101, 2023. doi: 10.1103/PhysRevLett.131.154101.

Pino, N. A., Convertito, V., Godano, C., and Piromallo, C. Subduction age and stress state control on seismicity in the NW Pacific subducting plate. *Sci. Rep.*, 12, 2022. doi: 10.1038/s41598-022-16076-8.

Roberts, N. S., Bell, A. F., and Main, I. G. Are volcanic seismic

b-values high, and if so when? *Journal of Volcanology and Geothermal Research*, 308:127–141, 2015. doi: 10.1016/j.jvolgeores.2015.10.021.

Rydelek, P. A. and Sacks, I. S. Testing the completeness of earthquake catalogs and the hypothesis of self-similarity. *Nature*, 337:251–253, 1989. doi: 10.1038/337251a0.

Scholz, C. The frequency-magnitude relation of microfracturing in rock and its relation to earthquakes. *Bull. seism. Soc. Am.*, 58: 399–415, 1968. doi: 10.1785/BSSA0580010399.

Taroni, M., Zhuang, J., and Marzocchi, W. High-Definition Mapping of the Gutenberg–Richter b-Value and Its Relevance: A Case Study in Italy. *Seismological Research Letters*, XX:1–7, 2021. doi: https://doi.org/10.1785/0220210017.

Tormann, T., Wiemer, S., and Mignan, A. Systematic survey of high-resolution b value imaging along Californian faults: Inference on asperities. *Journal of Geophysical Research: Solid Earth*, 119 (3):2029–2054, 2014. doi: 10.1002/2013JB010867.

Tramelli, A., Troise, C., De Natale, G., and Orazi, M. A new method for optimization and testing of microseismic networks: an application to Campi Flegrei (Southern Italy). *Bulletin of the Seismological Society of America*, 103(3):1679–1691, 2013. doi: 10.1785/0120120211.

Tramelli, A., Godano, C., Ricciolino, P., Giudicepietro, F., Caliro, S., Orazi, M., De Martino, P., and Chiodini, G. Statistics of seismicity to investigate the Campi Flegrei caldera unrest. *Scientific reports*, 11(1):7211, 2021. doi: 10.1038/s41598-021-86506-6.

Utsu, T. and Seki, A. A relation between the area of aftershock region and the energy of mainshock. *J. Seismol. Soc. Jpn.*, 7:233 – 240, 1954.

van der Elst, N. J. B-Positive: A Robust Estimator of Aftershock Magnitude Distribution in Transiently Incomplete Catalogs. *Journal of Geophysical Research: Solid Earth*, 126(2):e2020JB021027, 2021. doi: 10.1029/2020JB021027.

Wiemer, S. A Software Package to Analyze Seismicity: ZMAP. *Seismological Research Letters*, 72(3):373–382, 05 2001. doi: 10.1785/gssrl.72.3.373.

Wiemer, S. and Wyss, M. Mapping the frequency-magnitude distribution in asperities: An improved technique to calculate recurrence times? *J. Geophys. Res.*, 102:15,115–15,128, 1997. doi: 10.1029/97JB00726.

Wiemer, S. and Wyss, M. Minimum Magnitude of Completeness in Earthquake Catalogs: Examples from Alaska, the Western United States, and Japan. *Bulletin of the Seismological Society of America*, 90(4):859–869, 2000. doi: 10.1785/0119990114.

Wiemer, S. and Wyss, M. Mapping spatial variability of the frequency-magnitude distribution of earthquakes. *Adv. Geophys.*, 45:259–302, 2002. doi: 10.1016/S0065-2687(02)80007-3.

Wyss, M. Towards a Physical Understanding of the Earthquake Frequency Distribution. *Geophysical Journal of the Royal Astronomical Society*, 31(4):341–359, 1973. doi: 10.1111/j.1365-246X.1973.tb06506.x.

Y., O. Estimation of the Parameters in the Modified Omori Formula for Aftershock Frequencies by the Maximum Likelihood Procedure. *Journal of Physics of the Earth*, 31(2):115–124, 1983.

Zhuang, J. Next-day earthquake forecasts for the Japan region generated by the ETAS model. *Earth Planets and Space*, 63: 207–216, 2011. doi: doi.org/10.5047/eps.2010.12.010.

Zhuang, J. Long-term earthquake forecasts based on the epidemic-type aftershock sequence (ETAS) model for short-term clustering. *Research in Geophysics*, 2, 2012. doi: 10.4081/rg.2012.e8.

Zhuang, J. and Touati, S. Stochastic simulation of earthquake catalogs. *Community Online Resource for Statistical Seismicity Analysis*, 2015.

Zhuang, J., Ogata, Y., and Vere-Jones, D. Analyzing earthquake clustering features by using stochastic reconstruction. *Journal of Geophysical Research: Solid Earth*, 109(B5), 2004. doi: 10.1029/2003JB002879.